ARTICLE

Supplementary Information

Facile integration of single crystalline phthalocyanine nanowires and nanotrees as photoenhanced conductometric sensors

A. Nicolás Filippin,[a] Ángel Campos-Lendinez,[a] Juan Delgado-Alvarez,[a] Gloria Moreno-Martinez,[a] Javier Castillo-Seoane,[a] Víctor J. Rico,[a] Vanda F. Godinho, Ángel Barranco,[a] Juan R. Sanchez-Valencia,[a]* Ana Borras[a]*

Nanotechnology on Surfaces and Plasma Lab, Institute of Materials Science of Seville (CSIC-US), Americo Vespucio 49, 41092 Seville, Spain

Contact email: jrsanchez@icmse.csic.es, anaisabel.borras@icmse.csic.es

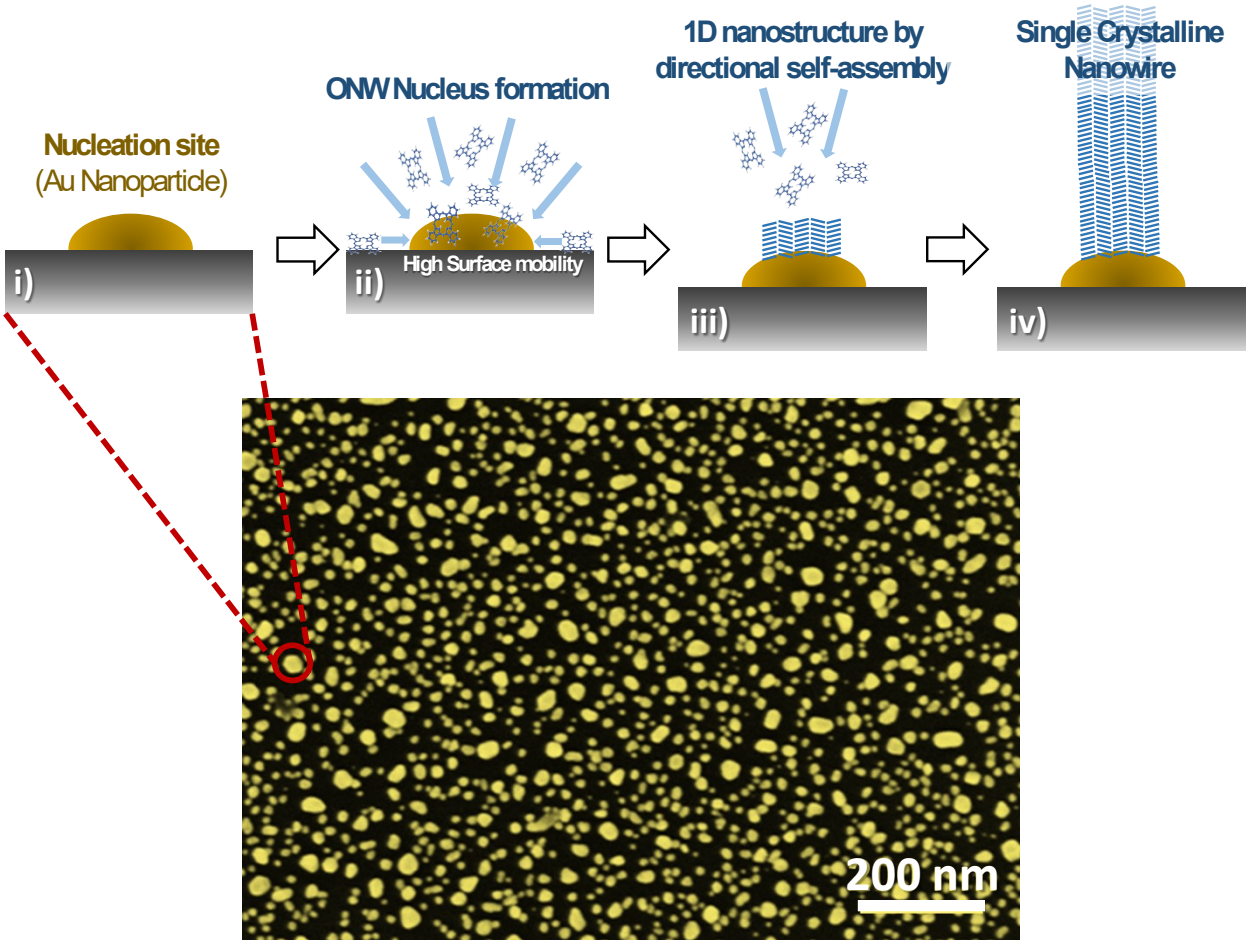

Figure S1. Top) Scheme of the growth of ONWs: i) nucleation sites on the substrates, in this case, gold nanoparticles.; ii) flux of molecules approaching the surface in an appropriate concentration and sufficient surficial molecular diffusion to reach the nucleation sites.; iii) formation of the crystal by self-assembly of the molecules directed by the π-stacking; iv) development of the nanowire. Bottom) SEM normal view of Au NPs used for the growth of the NWs, sputtering for 12.5 mA 10 s.

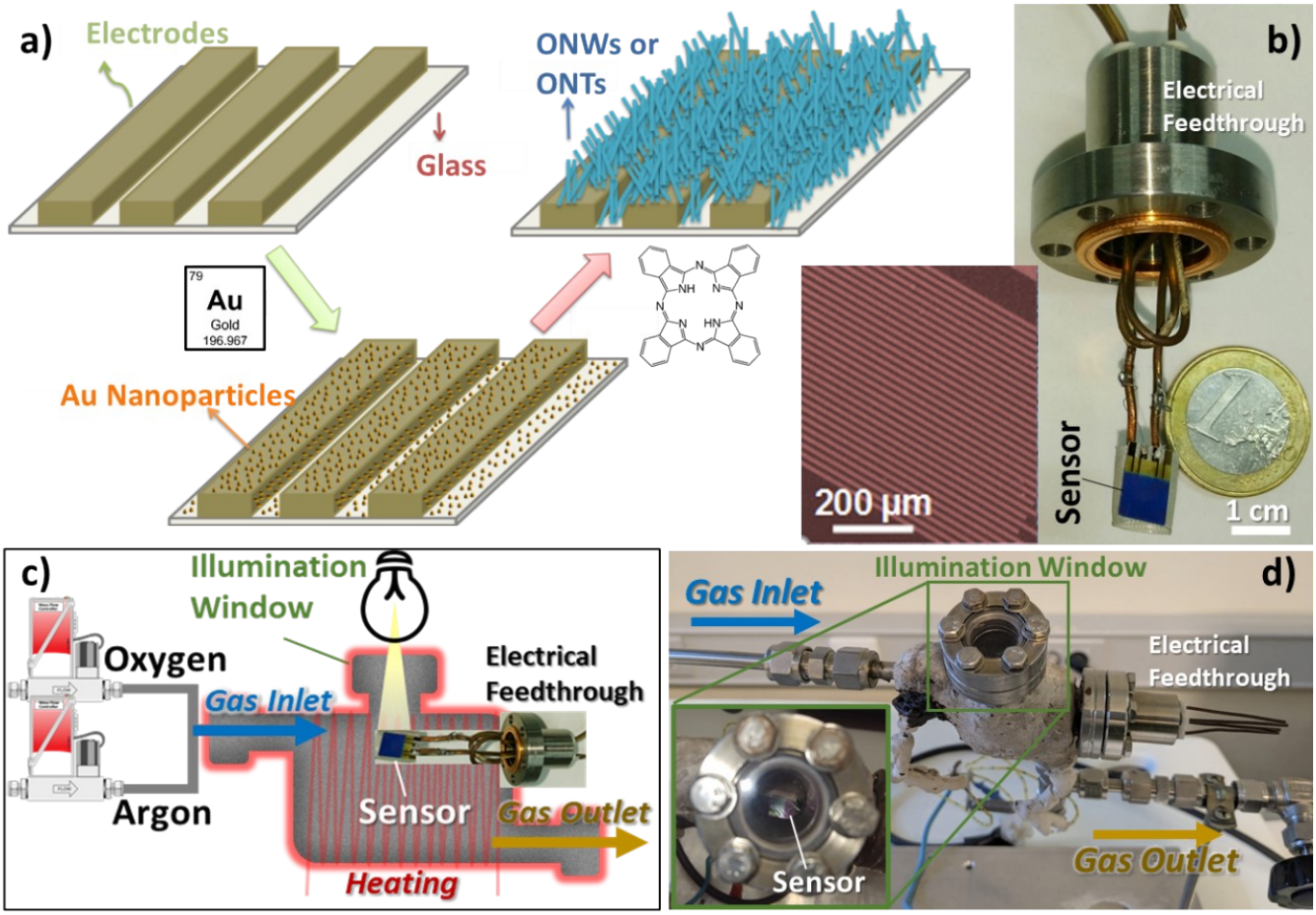

Scheme S1. a) Schematic on the deposition of organic nanowires onto preformed electrodes, formation of Au NPs by magnetron sputtering, and growth of single crystalline organic nanowires by physical vapour deposition of metal-free phthalocyanine (H_2Pc). b) Photograph of the final sensor device with the commercial electrodes decorated with ONWs attached to the feedthrough of the sensor characterization chamber. The inset shows a low-magnification SEM micrograph of the interdigitated electrodes. c-d) Scheme (c) and picture (d) of the sensor setup, highlighting all the relevant parts. Panel d) also shows a higher magnification picture with the view through the illumination window.

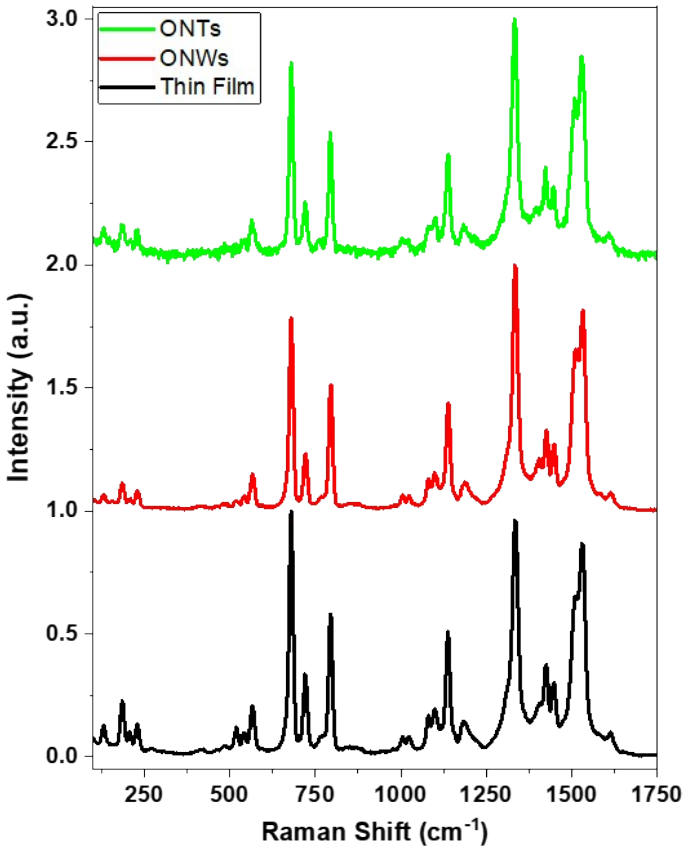

Figure S2. Normalised Raman spectra of a thin film obtained via sublimation of the H_2Pc precursor onto substrates at room temperature (RT, black line) and onto substrates annealed at 170°C during deposition, the temperature required for organic nanowires (ONWs) growth (red line). The corresponding Raman spectra exhibit a highly similar pattern, with the characteristic Raman peaks reported in the literature.[1] The figure includes the Raman spectrum of the organic nanotrees (ONTs, green line), synthesised through a deposition process analogous to the ONWs, with the key difference being an oxygen plasma treatment applied on the primary branches. This treatment facilitates the subsequent growth of additional ONWs (secondary branches) at defect sites introduced by the plasma. The ONTs display a slightly noisier Raman spectrum, likely due to surface amorphisation induced by the soft plasma treatment, which does not affect the inner core of the wires (see also TEM characterisation of ONTs provided in Figure 2 b) in the manuscript). Nevertheless, the spectrum shows the same features as the thin film and ONWs samples.

S3. X-Ray Photoelectron Spectroscopy (XPS) characterisation.

Figure S3 a) shows the survey spectra for ONW and ONTs samples, where the major elements present are C, N, and O. A small amount of Si (from the substrate) and gold can be noted, but the concentration is minimal. The elemental quantification (removing the small contribution from Si and Au) is shown in the Table in panel a). For the ONW, a very similar atomic concentration can be noted to that expected from the formula, with a slight deviation in the C to N ratio (C:N=5.1) which can be ascribed to hydrocarbon species adsorbed from the atmosphere. This ratio is further enhanced for the ONTs (C:N=5.5), likely linked to the generation of reactive surface radicals after the plasma treatment, which further favours the adsorption of hydrocarbon species after surface exposition rather than a preferential removal of N atoms with the Oxygen Plasma treatment.[2] However, the most significant difference lies in the oxygen content of the layers, which for the ONTs is increased to four times that of the ONWs.

Figure S3 also shows the zone spectra for C1s (b,e), N1s (c,f), and O1s (d,g) for both ONWs (b-d) and ONTs (e-g). The deconvolution of the C1s and N1s has been performed following the previous literature about the XPS of H_2Pc precursor.[3,4] All the spectral fitting was performed using the software CASA XPS. A Shirley background has been first removed from the spectra, and the main components have been fitted with a combination of Gaussian + Lorentzian

(30+70%). A tail at high binding energy (ca. 292 eV and 405 eV for C1s and N1s, respectively) can be noted, which is associated with inelastic electron scattering.[3]

According to the literature,[3] the C 1s spectra (panels b and e) of H_2Pc can be deconvoluted into distinct components corresponding to specific carbon chemical environments. The peak at 284.8 eV is attributed to benzene-type carbon atoms, while the signal at 286.3 eV corresponds to pyrrole-type carbon, along with shake-up structures associated with benzene carbon atoms. Additionally, a peak at 288.3 eV is linked to shake-up transitions of pyrrole carbon atoms. An additional minor peak at 287.8 eV is required to account for the presence of adsorbed carbonates from the atmosphere, exhibiting very low intensity. As observed in panels b, e), the spectral components used for fitting both ONWs and ONTs remain identical in binding energy positions, with only slight variations in the intensity of the higher binding energy components.

More pronounced differences are observed in the N 1s spectra (panels c and f), which have been deconvoluted into three primary components according to the literature.[3] The 398.9 eV and 400.4 eV peaks are associated with two-fold and three-fold coordinated nitrogen atoms within the H_2Pc molecule, respectively, while the peak at 402.7 eV is attributed to shake-up transitions. A notable difference between the ONW and ONT samples is the relative intensity of these components. Specifically, the ONTs exhibit a reduction in the peak corresponding to three-fold coordinated nitrogen, accompanied by an increase in the intensity of peaks at higher binding energies. While the high-energy peak is initially attributed to nitrogen shake-up transitions from the H_2Pc molecule, exposure to oxygen plasma is expected to induce oxidation, forming more oxidised nitrogen species. Therefore, the observed differences in N 1s peak shapes are likely a result of plasma-induced oxidation, particularly affecting three-fold coordinated nitrogen atoms.

The O 1s signal (panels d and g) shows a notable increase in intensity for ONTs compared to ONWs, consistent with the trends observed in the survey spectrum (panel a). Furthermore, the peak is slightly shifted to lower binding energies by approximately 0.3 eV. However, the deconvolution of the O 1s spectra does not yield significant insight, as a direct comparison between ONWs and ONTs is limited. This limitation arises because the O 1s signal in ONWs primarily originates from physisorbed species on the phthalocyanine wires, rendering it less relevant for comparative analysis.

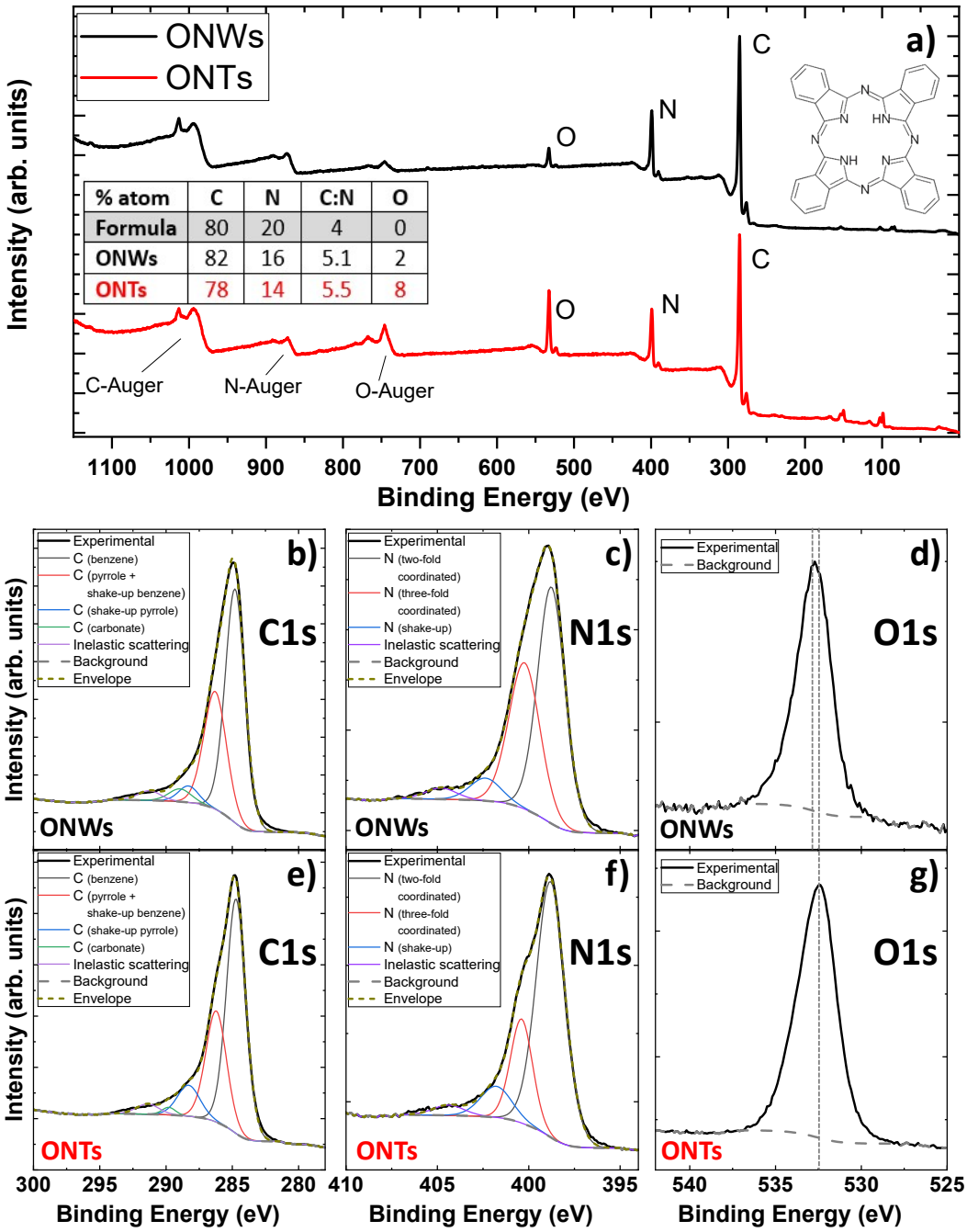

% atom	C	N	C:N	O
Formula	80	20	4	0
ONWs	82	16	5.1	2
ONTs	78	14	5.5	8

Figure S3. XPS spectra of ONWs (a, b-d) and ONTs (a, e-f). a) Survey spectra for both samples, which allow for identifying the major elements present (C, N and O). The panel also shows the elemental quantification (removing the small contribution from Si and Au). The figure also shows the detailed zone spectra for C1s (b,e), N1s (c,f), and O1s (d,g) for both ONWs (b-d) and ONTs (e-g).

S4. Estimation of the number of contacts between adjacent nanowires

First, the resistivity of the ONW needs to be considered. As mentioned in the main manuscript, to our knowledge, the resistivity of single-crystalline H_2Pc nanowires have not been reported. Assuming that the resistivity of the ONWs is similar to the dark resistivity reported for H_2Pc thin films (of around $10^6 \Omega\, m$ for a crystalline film with a thickness of 350 nm),[5] the expected resistance for a single H_2Pc ONW (with a diameter of 100 nm and a length of 10 um) should be around $R_{Single\ ONW} \approx 10^{15}\Omega$. Since the observed

resistance at RT for ONWs is $R_{ONWs} = 18.7 \cdot 10^9\ \Omega$, it would indicate that at least 50 thousands of ONWs are contacting the metallic interdigitated electrodes. Figure S2 shows a representative large-area statistical analysis of a top-view SEM image, which shows that the length of the ONW (most of the ONWs have lengths between 8-14 µm) is sufficient to make a possible contact with a neighbour nanowire growing from the immediately opposite electrode in the interdigitated structure (remember that the separation between electrodes is 10 µm). From the Figure S2 is also important to note the density of nanowires, which is around 1 ONW µm^{-2}. Considering than only the ONWs growing from the half of every electrode (5 µm of width) can contact their neighbour nanowires, it can be deduced that around the 20 % of the ONWs make a good electrical contact. This is a very high number since the calculated resistance value has been considered for a perfect ohmic contact between the ONWs, and the ones with a non-ideal connection would not contribute to the current flow.

This extrapolation is based on several assumptions, including that the resistivity of the ONWs is similar to the dark resistivity reported for H_2Pc thin films,[5] which does not fully account for the potential differences in crystallinity between nanowires and thin films. The higher crystallinity of individual nanowires likely results in lower resistance than calculated based on thin-film values. Thus, these calculations can only be considered a preliminary approximation to contextualize the results within the broader literature.

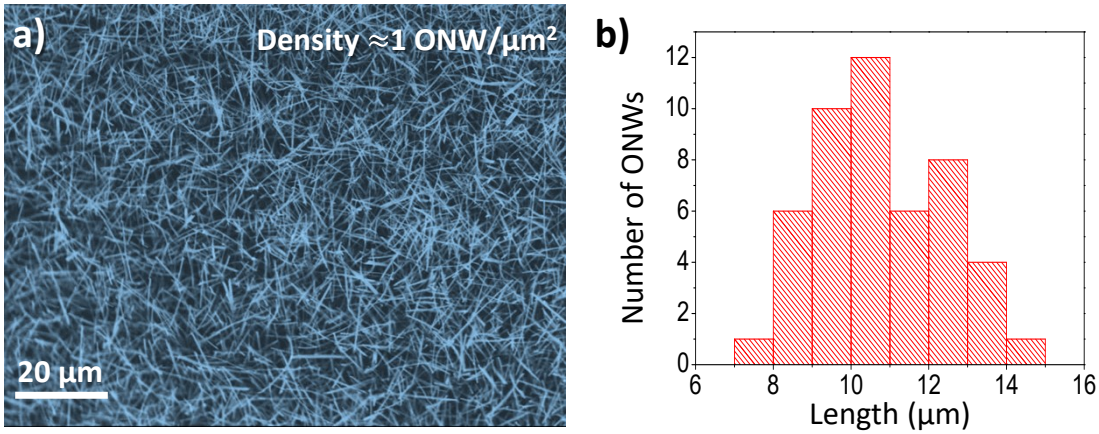

Figure S4. a) Surface SEM image of H_2Pc ONWs grown on Au NPs on Si wafer. b) Histogram of the number of ONWs vs Length, showing that most have a length from 8-14 µm.

Table S1. Resistance values of three different ONTs-based sensor devices deposited in different batches. The resistance values have been extracted from the IV curves measured at RT under Ar flux (for more than 10 minutes).

	Resistance (GΩ)
ONT-1	57.6 ± 8.6
ONT-2	23.3 ± 7.0
ONT-3	20.6 ± 7.1

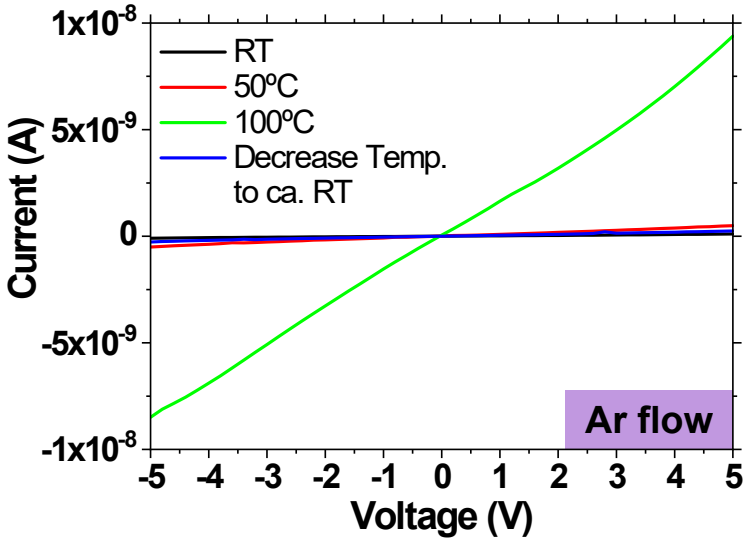

Figure S5. I-V curves for Nanotrees deposited on commercial electrodes at Room Temperature (black), 50 (red) and 100ºC (green) under constant argon flux at ambient pressure. The blue curve shows the recovery of the I-V characteristics after cooling down to a temperature of ca. RT.

Table S2. Power densities at a distance of 5 cm for the Xenon lamp with no filters (UV+Vis) and with a long-pass UV filter (Visible) and for the tree LEDS used for the illumination experiments. Values are expressed in mW/cm^2.

Light source	UVA+UVB (280-400 nm)	Vis+NIR (400-2500 nm)	UV+Vis+NIR (280-2500 nm)
Xenon lamp	42.8	1730	**1772.8**
Xenon lamp + Longpass filter	0	1700	**1700**
RED LED	0	5.38	**5.38**
GREEN LED	0	2.93	**2.93**
BLUE LED	0	2.89	**2.89**
WHITE LED (SUM OF R+G+B)	0	11.2	**11.2**

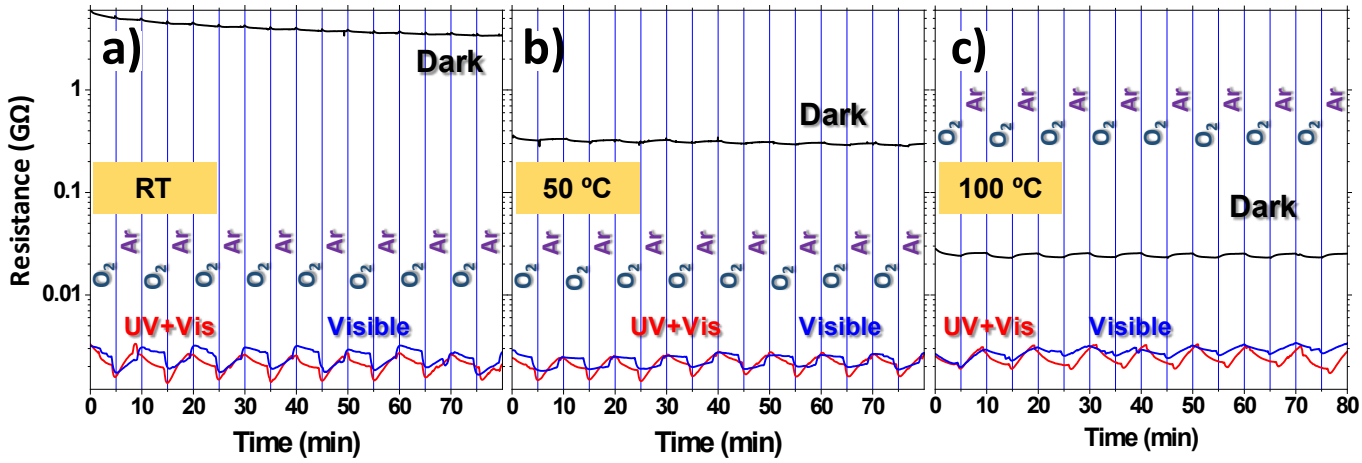

Figure S6. Sensor response to oxygen and argon in the range RT-100 ºC under no irradiation (black), visible light (green) and UV+visible light (red).

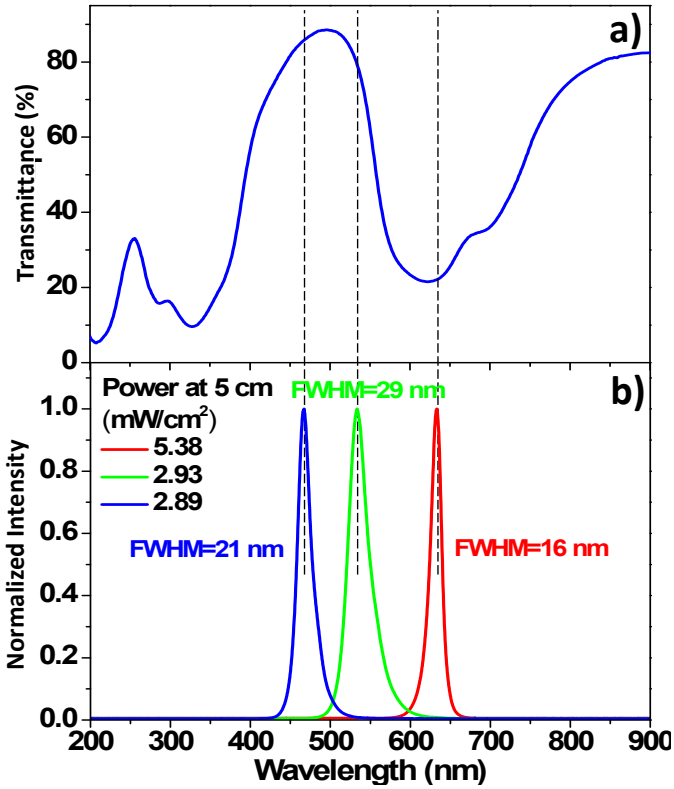

Figure S7. Transmittance spectrum of H_2Pc ONWs (a) and spectral distribution of the red, green and blue LEDs used for the illumination experiments (b).

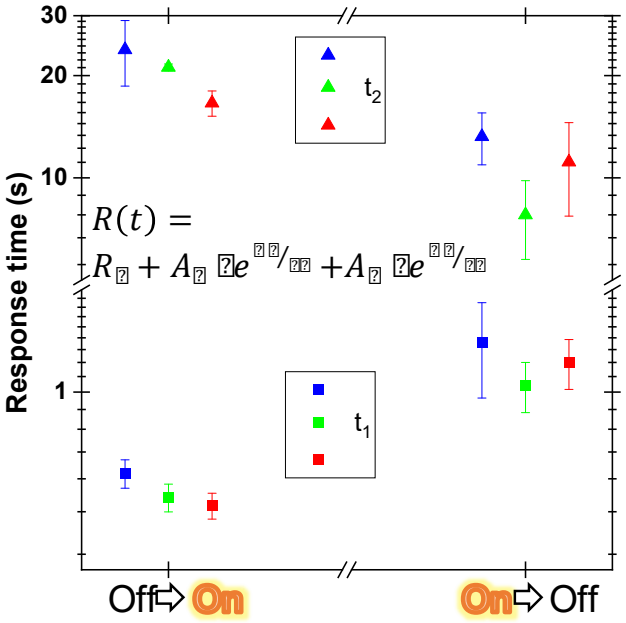

Figure S8. Response times fitted from the curves shown in Figure 6 a) for the three LEDs (blue, green, and red symbols), for both "Off-On" and "On-Off" transitions. A two-exponential decay was required for the fittings, by using the expression in the figure. In order to neutralize the effect of the drift, the fitting was performed using the first 30 seconds. Similar response times were observed, with two distinct components: t1 (faster) and t2 (slower). The response times differed significantly between the "Off-On" and "On-Off" transitions, with the

latter showing slower t1 and faster t2. The highest relative amplitude was obtained for t2 (more than 95% for all cases) and the faster time was required to fit the very fast initial step in the curves. As drift may influence the fits, the response times should be interpreted qualitatively.

References

1 A. A. El-Saady, N. Roushdy, A. A. M. Farag, M. M. El-Nahass and D. M. Abdel Basset, *Opt Quant Electron*, 2023, **55**, 662.
2 J. M. Obrero, A. N. Filippin, M. Alcaire, J. R. Sanchez-Valencia, M. Jacob, C. Matei, F. J. Aparicio, M. Macias-Montero, T. C. Rojas, J. P. Espinos, Z. Saghi, A. Barranco and A. Borras, *Frontiers in Chemistry*, DOI:10.3389/fchem.2020.00520.
3 Y. Alfredsson, B. Brena, K. Nilson, J. Åhlund, L. Kjeldgaard, M. Nyberg, Y. Luo, N. Mårtensson, A. Sandell, C. Puglia and H. Siegbahn, *The Journal of Chemical Physics*, 2005, **122**, 214723.
4 K. Nilson, J. Åhlund, M.-N. Shariati, J. Schiessling, P. Palmgren, B. Brena, E. Göthelid, F. Hennies, Y. Huismans, F. Evangelista, P. Rudolf, M. Göthelid, N. Mårtensson and C. Puglia, *The Journal of Chemical Physics*, 2012, **137**, 044708.
5 M. M. El-Nahass, A. M. Farid, A. A. Attia and H. A. M. Ali, *Applied Surface Science*, 2006, **252**, 7553–7561.